This document is the accepted manuscript version of the following article:
Cuny, H. E., Fonti, P., Rathgeber, C. B. K., von Arx, G., Peters, R. L., & Frank, D. C. (2019). Couplings in cell differentiation kinetics mitigate air temperature influence on conifer wood anatomy. Plant, Cell and Environment, 42, 1222-1232. https://doi.org/10.1111/pce.13464

Couplings in cell differentiation kinetics mitigate air temperature influence on conifer wood anatomy

Henri E. Cuny[1,2], Patrick Fonti[1,*], Cyrille B.K. Rathgeber[3], Georg von Arx[1], Richard L. Peters[1,4], David Frank[1,5]

[1] *Swiss Federal Research Institute WSL, CH-8903 Birmensdorf, Switzerland*
[2] *IGN, Direction Interrégionale Nord-Est, 54115 Champigneulles, France*
[3] *UMR LERFoB, AgroParisTech, INRA, 54000, Nancy, France*
[4] *Botanik, Basel University, CH-4056 Basel, Switzerland*
[5] *Laboratory of Tree-Ring Research, University of Arizona, 1215 E Lowell St, Tucson, AZ 85721, USA*

*** Corresponding author**: Patrick Fonti, patrick.fonti@wsl.ch, +41 44 739 22 85

Short title: Cell kinetics mitigate influence on conifer wood

Abstract

Conifer trees possess a typical anatomical tree-ring structure characterized by a transition from large and thin-walled earlywood tracheids to narrow and thick-walled latewood tracheids. However, little is known on how this characteristic structure is maintained across contrasting environmental conditions, due to its crucial role to ensure sap ascent and mechanical support.

In this study we monitored weekly wood cell formation for up to seven years in two temperate conifer species (i.e.; *Picea abies* (L.) Karst and *Larix decidua* Mill.) across an 8 °C thermal gradient from 800 to 2200 m a.s.l. in central Europe to investigate the impact of air temperature on rate and duration of wood cell formation.

Results indicated that towards colder sites, forming tracheids compensate a decreased rate of differentiation (cell enlarging and wall thickening) by an extended duration, except for the last cells of the latewood in the wall-thickening phase.

This compensation allows conifer trees to mitigate the influence of air temperature on the final tree-ring structure, with important implications for the functioning and resilience of the xylem to varying environmental conditions. The disappearing compensation in the thickening latewood cells might also explain the higher climatic sensitivity usually found in maximum latewood density.

Keywords

Wood formation dynamics; Conifer; Temperature response; Quantitative wood anatomy; Tree ring; Xylogenesis

Introduction

Conifers display an extraordinary biogeography with more than 600 species widely distributed across the globe: from the latitudinal limits of tree growth in the Northern and Southern Hemispheres to the Equator; from lowland savannas to near the perpetual snow line of the highest mountains; and from the wet forests of Alaska to the central Sahara (Farjon & Filer, 2013). Despite growing in very contrasting environments, conifers generally develop similar tree-ring structures (Schoch, Heller, Schweingruber & Kienast, 2004). Tracheids — the cells that provide both water transport and mechanical support and in conifers represent about 90% of wood or xylem tissue — are characterized by a seasonal transition in their dimensions. In wood produced during the early part of the growing season (earlywood), the tracheids are large with thin cell walls, whereas wood produced at the end of the growing season (latewood), is characterized by narrow, thick-walled tracheids. In short, a continuous seasonal transition in cell size and wall thickness is characteristic of conifers (Cuny, Rathgeber, Frank, Fonti & Fournier, 2014, Schoch *et al.*, 2004). This typical tree-ring structure reflects structural and physiological trade-offs that are important for tree functioning and performance. Wider tracheids are more efficient in transporting water but more prone to cavitation, while narrower thick-walled tracheids provide most of the mechanical support, yet are less efficient in transporting water (Chave, Coomes, Jansen, Lewis, Swenson & Zanne, 2009).

To date, most studies dealing with the influence of environment on wood formation (*i.e.* xylogenesis) have focused on its phenology, that is, the seasonal timings of the beginning, end and duration of cambial activity and wood formation (Deslauriers, Rossi, Anfodillo & Saracino, 2008, Rossi et al., 2016, Rossi, Deslauriers, Anfodillo & Carraro, 2007, Rossi, Deslauriers, Gričar, Seo, Rathgeber, Anfodillo, Morin, Levanic, Oven & Jalkanen, 2008). Such studies have revealed the strong plasticity of this aspect in response to air temperature variations: *e.g.*, towards colder environments growing season is shorter because wood formation starts later and ends earlier. But much less is known on how tree-ring structure is shaped during xylogenesis beyond the dependence upon kinetics of xylem cell differentiation processes: namely, the duration and rate of cell enlargement determine the final size of a xylem cell, while the duration and rate of wall thickening govern its final density. The contribution of each kinetic parameter in shaping the typical tree-ring structure has been recently quantified for temperate coniferous species (Cuny *et al.*, 2014, Rathgeber, Cuny &

Fonti, 2016). Yet, it remains unknown how these kinetic parameters may or may not vary across changing environments to maintain efficient wood tissues.

Here, we investigate how xylogenesis shapes conifer tree-ring structure across contrasting thermal environments. For this purpose, we gathered up to seven years of data on wood formation dynamics and xylem anatomy for two coniferous species — Norway spruce (*Picea abies* L.) and European Larch (*Larix decidua* Mill.) — along a ~2000 m elevation gradient in western Europe (Figure S1). The elevation gradient corresponds to a range of 8 °C in mean annual temperature (Table 1). We used a novel modeling approach to associate cell differentiation kinetics and final cell dimensions with the corresponding thermal conditions (Cuny & Rathgeber, 2016) (Figure S2). We establish the following three hypotheses: H1) lower site temperature is associated with a later start, earlier ending and shorter duration of xylem tissue formation; H2) due to these adjustments in phenology, the first and last xylem cells formed in the growing season experience more similar thermal conditions during their differentiation along the thermal gradient; H3) consequently, the kinetics (rates and durations) of the cell differentiation processes (cell enlargement and wall thickening), which determine the final dimensions of xylem cells, and thus shape the tree-ring structure, are quite similar despite contrasted thermal environments.

Material and Methods

Study area

The research was conducted at two main locations: one in the Lötschental valley (LTAL), in the Swiss inner Alps (46°23'N, 7°45'E), and one in the Donon (DNN), in the Vosges Mountains in northeast France (48°35'N, 7°08'E; Figure S1). In total, the research design included 12 sites (nine at the LTAL and three at the DNN) covering a wide range of air temperature, with a difference of about 8 °C between the mean annual temperatures of the coldest (2.2 °C) and the warmest sites (10.3 °C; Table 1).

The nine sites of the LTAL were selected along a 1400 m elevational transect (from 800 to 2200 m a.s.l.) including both north and south aspects (Figure S1). At 1300 m a.s.l. two sites were chosen on the same north aspect, with one site presenting particularly wet conditions (N13W). At each site of the LTAL, Norway spruce (*Picea abies* (L.) Karst.) and European Larch (*Larix decidua* Mill.) grow in inter-mixed stands, with the exception of the highest sites (N22 and S22) where only Larch is present. In the DNN, the three sites were selected along a

300 m elevational gradient (from about 350 to 650 m a.s.l.; Figure S1). At each of these sites, Norway spruce grows in mixed coniferous stands.

Sampling, preparation, and microscopic observations of xylem development

Xylogenesis was monitored during three years in DNN (2007-2009) and up to seven years in the LTAL (2007-2013), depending on the site (Table 1). On each site, three to four (in LTAL) or five (in DNN) mature and dominant trees per species (Norway spruce at DNN; Norway spruce and European larch at LTAL) were monitored each year. In the LTAL, because of the long-term monitoring performed, the monitored trees were changed after the 2007, 2009, and 2011 growing seasons in order to reduce impact of sampling-related wound reaction. In the DNN, the same five trees were monitored during the three years.

The assessment of the timing of tracheid formation was based on repeated cellular observations performed on micro-cores taken over the full growing season at different position around the stem circumference. Microcores were collected weekly at breast height (1.3 m) on the trunk of the selected trees from April to November, using a Trephor tool (Rossi, Anfodillo & Menardi, 2006a). Successive microcores were then taken at least 1 cm apart from each other and following a slightly ascending spiral pattern to avoid wound reaction. Microcores were then prepared in the laboratory, and 5–15 µm-thick transverse sections were cut with a microtome. Sections were stained (with cresyl violet acetate at DNN, safranin and astrablue at LTAL) and permanently mounted on glass slides (Rossi, Deslauriers & Anfodillo, 2006b). Xylogenesis observations were performed on the sections using an optical microscope under visible and polarized light at ×100–400 magnification to distinguish the different phases of development among the cells. Thin-walled enlarging cells were distinguished from cambial cells by their larger size. Cells in the thickening zone developed secondary walls that could be detected under polarized light because of the orientation of cellulose microfibrils (Abe, Funada, Ohtani & Fukazawa, 1997). Staining was used to follow the advancement of lignification (Rossi *et al.*, 2006b). Thickening cells exhibited two-colored walls indicating that lignification was in progress, whereas mature tracheids presented entirely lignified and thus monochromatic walls.

Count data of cells in different xylogenesis phases were standardized by the total number of cells of the previous ring (Rossi, Deslauriers & Morin, 2003) using the R package *CAVIAR* (Rathgeber, 2012). This standardization process reduces the noise in the data, thus increasing the signal-to-noise ratio by about 50% (Cuny *et al.*, 2014).

Quantitative wood anatomy

For each tree, anatomical sections from microcores (DNN) or from standard 5 mm cores (LTAL) taken after the end of the growing season were used to characterize the structure of the tree rings produced during the monitoring period. Digital images of the tree rings were analyzed using image analysis software specifically developed for wood cell analysis in order to measure the dimensions of tracheids along radial files. The WinCell software (Regent instruments, Canada) was used for trees at DNN to measure cell dimensions along an average of five radial files per tree; and ROXAS (von Arx & Carrer, 2014, Prendin, Petit, Carrer, Fonti, Björklund & von Arx, 2017) and RAPTOR (Peters *et al*., 2017) was used for trees at LTAL to measure cell dimensions along an average of 30 radial files. Both programs measure the radial and tangential lumen diameter, the lumen area and the wall thickness of each tracheid from transversal cuts. However, while WinCell measures only the tangential wall thickness, ROXAS measures both the tangential and the radial wall thicknesses. ROXAS measurements revealed that for both species the radial and tangential wall thicknesses were similar in earlywood, whereas in latewood the radial wall thickness is about 1.3 times larger. We therefore multiplied the tangential wall thickness values by this factor to estimate the radial wall thickness at DNN. From these anatomical variables, the cell and wall cross-sectional areas (CCA and WCA) were then calculated and considered as the final results of the differentiation phases of cell enlargement and wall deposition, respectively (Figure 1) (Cuny *et al.*, 2014).

To show variations in tracheid dimensions along a ring, individual cell morphological measurements were grouped by radial file in profiles called tracheidograms (Vaganov, 1990). Because the number of cells varied between radial files within and between trees, tracheidograms were standardized according to Vaganov's method (Vaganov, 1990) using a dedicated function of the R package *CAVIAR* (Rathgeber, 2012). This standardization allows adjusting the length of the profiles (cell numbers) without changing their shape (cell dimensions (Vaganov, 1990). We checked visually that this standardization didn't alter the shape of the anatomical profiles. The standardized tracheidograms were then averaged by site, year and species.

Mature tracheids were classified into three different types of wood: earlywood, transition wood and latewood; according to Mork's criterion (MC) (Denne, 1988), which is computed as the ratio between four times the tangential wall thickness divided by the radial lumen

diameter. Tracheids were classified as follows: MC ≤ 0.5, earlywood; 0.5 < MC < 1, transition wood (not further used in the analysis); MC ≥ 1, latewood (Figure 1) (Park & Spiecker, 2005).

Quantification of wood formation dynamics

In order to accurately characterize wood formation dynamics, generalized additive models (GAMs) were fitted on the standardized numbers of cells for each phase of xylem development, each year, and each individual tree (Cuny, Rathgeber, Kiesse, Hartmann, Barbeito & Fournier, 2013), using the R package *mgcv* (R Core Team, 2015, Wood, 2006). The predictions of the fitted models were then averaged in order to characterize the mean behavior of each species, during each year, and at each site.

Moreover, for each species, we used the average cell numbers predicted by GAMs to calculate the date of entrance of each cell in each differentiation zone (enlargement, wall thickening and mature) of xylem formation along the developing tree ring, following the method described in Cuny *et al.*, (2013) (Figure S2). From these dates, the duration of stay of each cell i in the enlargement ($d_{E,i}$) and wall thickening ($d_{W,i}$) zones were computed. For each cell i, we then estimated the rate of enlargement ($r_{E,i}$) and wall thickening ($r_{W,i}$) by dividing its final dimensions (CCA_i and WCA_i) by the duration ($d_{E,i}$ and $d_{W,i}$) it spent in the corresponding phase (enlargement and wall thickening) (Cuny *et al.*, 2014).

Meteorological data

In the LTAL, climatic conditions (air temperature, air relative humidity, soil moisture) were measured *in-situ* at each site beneath the canopy at 15-min intervals during the monitoring period. At the DNN, daily meteorological data (air temperature, precipitation, cumulative global radiation, wind speed, and air relative humidity) during the monitoring period were gathered from three meteorological stations distributed over the studied area, following the location of the selected sites. For every site, the soil relative extractable water (REW) was calculated. For the LTAL, the REW was directly calculated using the measurements of soil moisture and the soil depth. For the DNN, the REW was assessed with the model Biljou©, which takes as input the measured meteorological parameters along with several soil (*e.g.* number and depth of layers as well as proportion of fine roots per layer) and stand (forest type and maximum leaf area index) parameters, and gives as output the REW at a daily scale (Granier, Breda, Biron & Villette, 1999).

Air temperature influence on wood formation dynamics and tree-ring structure

In order to study accurately the mechanisms by which xylogenesis and tree-ring structure respond to air temperature, the kinetics of tracheid differentiation and the resulting dimensions of xylem cells were compared with the exact thermal conditions prevailing during the process of formation (Figure S2). Air temperature was used can be considered as a good indicator of cambium temperature (see Cuny & Rathgeber, 2016). For example, the kinetics of enlargement and the final cross-sectional area of a cell were compared to the mean air temperature experienced during the enlargement of this cell. Similarly, the kinetics of wall thickening and the final wall cross-sectional area of a given cell were compared to the mean air temperature it experienced during its wall thickening. Finally, the lumen area and wall thickness, which integrate both cell size and wall amount, were compared to the mean air temperature experienced during the whole period of cell differentiation (*i.e.* enlargement plus wall thickening).

As we wanted to focus on the variations in kinetics and anatomy according to the different thermal environments (*i.e.* sites), data (cell development kinetics, cell dimensions and associated thermal conditions) were averaged per site, species and also by separating earlywood and latewood cells in order to test the possibility of different environmental sensitivities between these two tree-ring zones. Transition wood was not included in order to focus only on clearly defined wood structures.

Then, relationships between mean thermal conditions, kinetics parameters (rate and duration of cell enlargement and wall thickening), and anatomical variables (cell area, lumen area, wall area, wall thickness) were assessed using linear models. Additionally, to account for possible biases for the assessment of the influence of air temperature on xylem cell dimension and kinetics due to missing independence of data caused by pseudo-replication (the same trees have been monitored for two to three consecutive years), mixed linear effect models with tree as random factor have been compared to linear models before averaging data per site and species. In particular, covariance analyses were performed to evaluate the effects of species (European larch and Norway spruce), wood types (earlywood and latewood), tree age and dimensions (height and diameter) on the relationships. Significant variables and interactions were identified by backward elimination using the R function drop1 (R Core Team, 2015), which allows selecting the best model based on the Akaike information criterion (AIC). The best model was chosen based on the higher AIC (difference >2) using the maximum likelihood method (Zuur, Ieno, Walker, Saveliev, & Smith, 2009). Analyses were performed

using r (version 3.1.1; R Development Core Team, 2014), and linear mixed-effects models were run using the lme4 (Bates, Mächler, Bolker, & Walker, 2015) and MuMIn packages (Barton & Barton, 2013). Finally, as the assessed kinetics and anatomical parameters are on different scales and have different absolute values between them and between early- and late-wood, relationships were also assessed on normalized data in order to compare the slopes between the different variables and wood types.

In order to test the effects of other potentially important climatic factors related to site hydric conditions, the same approach was employed using the soil relative extractable water instead of air temperature.

Implications of the xylogenesis response to thermal conditions for tree-ring structure and functions

To assess the implications of the xylogenesis response to thermal conditions in terms of tree-ring structure and associated functions, we used the relationships established to simulate the average kinetics and resulting dimensions of the cells produced at two theoretical sites representing a 5 °C gradient (~3.5 °C and 8.5 °C in average air temperature, respectively). For that, the relationships established between thermal conditions and kinetics parameters were used to simulate the rate and duration of differentiation processes for the two thermal modalities. The simulated kinetics were then used to calculate cell dimensions. For example, the cell cross-sectional area was calculated by multiplying the simulated rate and duration of cell enlargement, while the wall cross-sectional area was calculated by multiplying the simulated rate and duration of wall thickening. Other dimensions (lumen area, cell and lumen diameters, and wall thickness) could then be calculated from these two anatomical dimensions and used to build virtual cells assuming rectangular-shaped tracheids (Cuny *et al.*, 2014). Finally, the calculated cell dimensions were used to infer some indices about the functions (conductivity) and mechanical properties (cell reinforcement) associated to the simulated tracheids (Figure 1). Conductivity was thus calculated as the square of the lumen cross-sectional area according to Hagen-Poiseuille law (Sutera & Skalak, 1993), while the cell reinforcement was calculated according to (Hacke, Sperry, Pockman, Davis & McCulloch, 2001):

$$\text{Cell reinforcement} = \left(\frac{2\times \text{WTT}}{\text{LTD}}\right)^2,$$

where WTT is the tangential wall thickness and LTD the lumen tangential diameter (Figure 1).

Results

Wood formation phenology partially adjusts to the thermal environment

Our observations only partially confirmed our first hypothesis, namely the phenology of xylem tissue formation adjusts to thermal environment. We indeed found that along the gradient, the start of wood formation showed strong negative linear relationships with the mean annual temperature of the site ($P<0.001$, $n=19$; Figure 2; Table S2). For both species, the beginning of cell enlargement period was delayed by 4.7 days for a 1 °C decrease in temperature, whereas the beginnings of wall thickening and mature periods were delayed by 5.2 and 6.7 days, respectively (Figure 2). In contrast, the ending of wood formation phases did not show any statistical association with site temperature (Figure 2).

Air temperature during cell development varied widely between thermal environments

Contradicting the second hypothesis, despite the plasticity observed in phenology, xylem cell differentiation operated at different air temperatures along the gradient (Figure 3), even for the cells formed at the margin of the growing season (i.e., the first and last tracheid in the ring). For example, the air temperature during differentiation of the first cells varied by 5 °C across sites (Figure 3b). Similarly, a 6 °C range was observed for the air temperature experienced by earlywood cells (Figure 3c), whereas thermal differences exceeded 8 °C for latewood cells and approach 10 °C for the last cells in a ring (Figure 3d,e). These observations of air temperature differences, that generally increased when moving from early- to latewood cells even if we consider the maximum or minimum daily temperatures (data not shown), indicate that the delayed phenological onset at cold sites only partially buffered the gradient observed in mean annual temperature.

Air temperature strongly influenced cell development kinetics

Figure 4 shows the implications of thermal conditions for xylogenesis processes, which exhibited different kinetics along the gradient, thereby disproving our third hypothesis. Including pseudo-replication effect due to repeated observation over two to three years did not provided better model than linear model (data not shown). We found highly significant

associations between air temperature and the kinetics of cell differentiation processes ($P<0.001$, $n=38$; Table S4), whereas the hydric conditions had no effects (Figure S5). For both species, we found strong, positive, linear relationships between the mean air temperature experienced during process and the rates of this process (Figure 4a,b). However, we also observe strong, negative, linear relationships between air temperature and the durations of processes (Figure 4c,d). In fact, rates and durations were tightly linked (Figure 4e,f). Towards colder sites, decreasing rates were associated with increasing durations. For cell enlargement, this coupling operated similarly in earlywood and latewood (Figure 4e; but see also Figure S4e). In contrast, for wall thickening, coupling breaks down in latewood (Figure 4f).

The plasticity observed in cell kinetics mitigated air temperature influence on tree-ring structure

The observed compensation between rates and durations of xylogenesis processes mitigated air temperature effects on tree-ring structure, which displayed its characteristic pattern along the elevation gradient (Figure S6). Yet, thermal conditions still had a significant influence on final cell dimensions ($P<0.001$, $n=38$; Figure 5; Table S5), but this influence was modest compared to the observed effects on process kinetics (compare slopes of relationships on normalized data in Figures S4 and S7). Thus, we found consistent anatomical differences across the elevation gradient: tracheids had lower cross-sectional cell area (Figure 5a), wall area (Figure 5b), lumen area (Figure 5c), and wall thickness (Figure 5d) towards colder sites. Moreover, owing to the breakdown in rate-duration coupling for wall thickening, we observed a particularly high thermal sensitivity of wall area and thickness in latewood (Figure 5b,d).

Discussion

Nevertheless, this study reveals the high plasticity and complex interactions at play in the dynamic of wood formation in response to air temperature. Our results emphasized a tight coupling between the rates and the durations of xylem cell development processes: towards colder environments, the rates of cell enlargement and wall thickening decreased, but in parallel their durations increased. These differences observed along the thermal gradient might be also partially explained via differing thermal requirements as induced by processes of local adaptation, as observed in common garden experiment. However, previous studies on the genetic variation along elevation gradients performed on the same species considered here are suggesting that the plasticity observed here is rather a response to mean site climatology

than a genetic adaptation of tree populations to local conditions (King, Fonti, Nievergelt, Buntgen & Frank, 2013, Nardin et.al., 2015).

The dependency of the start of xylem tissue formation on air temperature observed in our study sites is consistent with previous reports for numerous other coniferous species in boreal (Rossi *et al.*, 2016, Rossi *et al.*, 2008), subalpine (Deslauriers *et al.*, 2008, Rossi *et al.*, 2007), temperate (Rossi *et al.*, 2016), and Mediterranean (Camarero, Olano & Parras, 2010) forest biomes. In contrast, environmental factors controlling cessation of wood formation remain unclear, even though temperature has also been recognized as an important driver across the Northern Hemisphere (Rossi *et al.*, 2016). At more local geographical scales, the ending dates of wood formation have been related to the number of cells produced (Lupi, Morin, Deslauriers & Rossi, 2010, Rossi, Morin & Deslauriers, 2012), but here we observed no connection between the wood formation phenology and the annual increment, which was mostly related to the cell production rate (Figure S3; Table S3). The observation that the ending of the growing season was stable across the thermal gradient suggests that in our sites photoperiod (Mellerowicz, Coleman, Riding & Little, 1992) is an important factor controlling the end of xylem tissue formation.

Concerning the control of the kinetics of cell differentiation processes, the rate and the duration have usually been considered separately. On the one hand, the control of the rate has been associated with a direct influence of temperature on metabolism (Balducci, Cuny, Rathgeber, Deslauriers, Giovannelli & Rossi, 2016, Cuny & Rathgeber, 2016, Cuny et al., 2015, Mellerowicz *et al.*, 1992, Proseus, Ortega & Boyer, 1999, Proseus, Zhu & Boyer, 2000). Cell enlargement implies numerous enzyme reactions (*e.g.* cutting chemical bonds to loosen the wall, synthesizing, transporting, delivering and inserting new wall polymers) with high activation energies, and thus likely being very sensitive to temperature (Proseus *et al.*, 1999, Proseus *et al.*, 2000), while the processes involved in wall thickening (*e.g.* cellulose and lignin biosynthesis, transport and deposition) are inhibited at temperatures still favorable for photosynthesis (Körner, 1998, Körner, 2003, Simard, Giovannelli, Treydte, Traversi, King, Frank & Fonti, 2013). On the other hand, the regulation of process duration has more commonly been associated with hormonal signaling (Schrader, Baba, May, Palme, Bennett, Bhalerao & Sandberg, 2003, Tuominen, Puech, Fink & Sundberg, 1997, Uggla, Moritz, Sandberg & Sundberg, 1996). A morphogenetic gradient of auxin concentration would shape the zonation of the developing xylem and govern process durations by providing positional information to differentiating cells (Tuominen *et al.*, 1997, Uggla *et al.*, 1996).

By revealing a tight coupling between the rate and the duration of xylogenesis processes, our results urge for a more integrated approach to understanding xylogenesis and its control, with the necessity to consider together all components of the dynamics of the system and their interactions. Indeed, to date the mechanisms coordinating the durations and rates of cell differentiation processes remain unknown. For wall thickening, a mechanism linking the rate of secondary wall deposition to the date of apoptosis may explain the observed coupling (Cuny & Rathgeber, 2016, Groover & Jones, 1999). But why and how this coupling is broken during latewood formation is still unexplained (Cuny *et al.*, 2014).

With regard to coupling, the question arises as to why conifers maintain such consistent tree-ring structure (earlywood, latewood) instead of, for example, adjusting the number of cells in a ring. This strategy makes sense when viewed from a functional standpoint, where a moderate change in tracheid dimensions can trigger a dramatic change in hydraulic functioning. For example, assuming tracheids behave as capillary tubes, the conductivity scales with the lumen diameter to the fourth power (Hagen-Poiseuille law; Sutera & Skalak, 1993). Hence, a two-fold decrease in lumen diameter implies a 16-fold decrease in conductivity. In other words, 16 cells would be needed to achieve the conductivity of a single cell having a two times wider lumen.

We used the relationships presented in Figure 4 to simulate the average dimensions and associated properties of tracheids at two theoretical sites (cold and warm) representing a 5 °C gradient. To assess the implications of the observed kinetics regulation, we then performed this exercise for the cold site, but using durations of the warm site. We estimate that without adjustment in the durations of cell differentiation processes, trees growing at the cold site would produce earlywood tracheids with approximately two times smaller lumen areas than at warm site, implying nearly a four-fold reduction in conductivity (Figure 6). In reality, the adjustments in duration of expansion allow producing cells with only 1.3 times smaller lumen areas and less than a two-fold reduction in conductivity. Simulations also reveal that duration adjustments allow increasing cell reinforcement and hydraulic safety of tracheids at the cold site (Figure 6). This makes sense with the necessity to increase resistance to frost-induced embolism by avoiding wall collapse under negative pressure (Charra-Vaskou, Badel, Charrier, Ponomarenko, Bonhomme, Foucat, Mayr & Améglio, 2016).

Despite the compensatory mechanisms at play in the kinetics of cell development processes, anatomical differences were observed between the different thermal environments: trees growing at colder sites produced xylem cells having smaller dimensions (cell area, wall area,

wall thickness, and lumen area). Moreover, because of the breakdown of the coupling between rates and durations of wall thickening, latewood tracheids were particularly sensitive to temperature. Such results contribute explaining why the maximal wood density — a dendrochronological parameter tightly connected to the anatomy of latewood tracheids — is particularly well related to temperature conditions and so useful as a proxy for paleoclimate reconstructions (Briffa, Schweingruber, Jones, Osborn, Shiyatov & Vaganov, 1998, Frank & Esper, 2005, Hughes, Schweingruber, Cartwright & Kelly, 1984).

Our study reveals and quantifies the strong response of xylogenesis kinetics to the thermal environment. The compensation observed between rates and durations of tracheid differentiation notably appears as an essential mechanism that allows conifers to cope with environmental change. In addition to its role in dealing with seasonal climatic variations (Cuny & Rathgeber, 2016) and mitigating the impacts of unusual extreme climatic events such as drought (Balducci *et al.*, 2016), we show that this rate-duration compensation preserves the characteristic tree-ring structure optimized for mechanical stability and water transport across a wide range of thermal conditions. This study thus provides new fundamental insights into tree growth, as well as mechanistic understanding of responses of trees to climate change.

Acknowledgements

We thank E. Cornu, E. Farré, J. Franzen, C. Freyburger, P. Gelhaye, Maryline Harroué, G. King, A. Mercanti, L. Moser, D. Nievergelt, L.Schneider, K. Treydte and A. Verstege for help in field- and lab-work; B. Longdoz, M. Nicolas and the association for the study and monitoring of air pollution in Alsace (ASPA) for supplying meteorological data. The authors acknowledge the Swiss National Science Foundation SNF (projects CLIMWOOD-160077 and LOTFOR-150205). GvA was supported by a grant from the Swiss State Secretariat for Education, Research and Innovation SERI (SBFI C14.0104). This research also benefited from the support of the FPS COST Action STReESS (FP1106).

Author Contributions

P.F. and D.F. designed the Swiss experimental setting; C.B.K.R. conceived the French experimental setting. H.E.C. collected the French sites data; P.F., R.L.P., G.v.A. and H.E.C. contributed to the data collection of the Swiss sites. H.E.C. performed the research and analyzed the data, with the contribution of all authors. H.E.C. wrote the manuscript and

prepared the figures, with the contribution of all authors. All authors discussed, reviewed and approved the manuscript.

Conflict of Interest

The authors declare that they have no conflict of interest.

Lay Summary

The structure of conifer's wood cells depends on speed and duration of processes shaping their formation. In this study we show for the first time that cells growing at colder sites increase their duration to compensate for a speed reduction. This compensation allows conifers mitigating the effect of air temperature to maintain a more similar tree-ring structure despite contrasted conditions.

References

Abe H., Funada R., Ohtani J. & Fukazawa K. (1997) Changes in the arrangement of cellulose microfibrils associated with the cessation of cell expansion in tracheids. *Trees-Structure and Function*, **11**, 328-332.

Balducci L., Cuny H.E., Rathgeber C.B.K., Deslauriers A., Giovannelli A. & Rossi S. (2016) Compensatory mechanisms mitigate the effect of warming and drought on wood formation. *Plant, Cell & Environment*, **39**, 1338-1352.

Barton K. & Barton M.K. (2013). MuMIn: multi-model interference. R Package version 1.9.5. Retrived from http://r-forge.r-project.org/ projects/mumin/10/6/2013

Bates D., Mächler M., Bolker B. & Walker S. (2015). Fitting linear mixed-effects models using lme4. *Journal of Statistical Software*, **67**, 1–48.

Briffa K.R., Schweingruber F.H., Jones P.D., Osborn T.J., Shiyatov S.G. & Vaganov E.A. (1998) Reduced sensitivity of recent tree-growth to temperature at high northern latitudes. *Nature*, **391**, 678-682.

Camarero J.J., Olano J.M. & Parras A. (2010) Plastic bimodal xylogenesis in conifers from continental Mediterranean climates. *New Phytologist*, **185**, 471-480.

Charra-Vaskou K., Badel E., Charrier G., Ponomarenko A., Bonhomme M., Foucat L., Mayr S. & Améglio T. (2016) Cavitation and water fluxes driven by ice water potential in *Juglans regia* during freeze–thaw cycles. *Journal of Experimental Botany*, **67**, 739-750.

Chave J., Coomes D., Jansen S., Lewis S.L., Swenson N.G. & Zanne A.E. (2009) Towards a worldwide wood economics spectrum. *Ecology Letters*, **12**, 351-366.

Cuny H.E. & Rathgeber C.B. (2016) Xylogenesis: coniferous trees of temperate forests are listening to the climate tale during the growing season but only remember the last words! *Plant Physiology*, **171**, 306-317.

Cuny H.E., Rathgeber C.B.K., Frank D., Fonti P. & Fournier M. (2014) Kinetics of tracheid development explain conifer tree-ring structure. *New Phytologist*, **203**, 1231-1241.

Cuny H.E., Rathgeber C.B.K., Frank D., Fonti P., Mäkinen H., Prislan P., Rossi S., del Castillo E.M., Campelo F., Vavrčík H., Camarero J.J., Bryukhanova M.V., Jyske T., Gričar J., Gryc V., De Luis M., Vieira J., Čufar K., Kirdyanov A.V., Oberhuber W., Treml V., Huang J.-G., Li X., Swidrak I., Deslauriers A., Liang E., Nöjd P., Gruber A., Nabais C., Morin H., Krause C., King G. & Fournier M. (2015) Woody biomass production lags stem-girth increase by over one month in coniferous forests. *Nature Plants*, **1**.

Cuny H.E., Rathgeber C.B.K., Kiesse T.S., Hartmann F.P., Barbeito I. & Fournier M. (2013) Generalized additive models reveal the intrinsic complexity of wood formation dynamics. *Journal of Experimental Botany*, **64**, 1983-1994.

Denne M.P. (1988) Definition of latewood according to Mork (1928). *Iawa Bulletin*, **10**, 59-62.

Deslauriers A., Rossi S., Anfodillo T. & Saracino A. (2008) Cambial phenology, wood formation and temperature thresholds in two contrasting years at high altitude in southern Italy. *Tree Physiology*, **28**, 863-871.

Farjon A. & Filer D. (2013) *An atlas of the world's conifers: an analysis of their distribution, biogeography, diversity and conservation status*. Brill.

Frank D. & Esper J. (2005) Characterization and climate response patterns of a high-elevation, multi-species tree-ring network in the European Alps. *Dendrochronologia*, **22**, 107-121.

Granier A., Breda N., Biron P. & Villette S. (1999) A lumped water balance model to evaluate duration and intensity of drought constraints in forest stands. *Ecological Modelling*, **116**, 269-283.

Groover A. & Jones A.M. (1999) Tracheary element differentiation uses a novel mechanism coordinating programmed cell death and secondary cell wall synthesis. *Plant Physiology*, **119**, 375-384.

Hacke U.G., Sperry J.S., Pockman W.T., Davis S.D. & McCulloch K.A. (2001) Trends in wood density and structure are linked to prevention of xylem implosion by negative pressure. *Oecologia*, **126**, 457-461.

Hughes M.K., Schweingruber F.H., Cartwright D. & Kelly P.M. (1984) July-August temperature at Edinburgh between 1721 and 1975 from tree-ring density and width data. *Nature*, **308**, 341-344.

King G., Fonti P., Nievergelt D., Buntgen U. & Frank D. (2013) Climatic drivers of hourly to yearly tree radius variations along a 6 degrees C natural warming gradient. *Agricultural and Forest Meteorology*, **168**, 36-46.

Körner C. (1998) A re-assessment of high elevation treeline positions and their explanation. *Oecologia*, **115**, 445-459.

Körner C. (2003) Carbon limitation in trees. *Journal of Ecology*, **91**, 4-17.

Lupi C., Morin H., Deslauriers A. & Rossi S. (2010) Xylem phenology and wood production: resolving the chicken-or-egg dilemma. *Plant Cell and Environment*, **33**, 1721-1730.

Mellerowicz E., Coleman W., Riding R. & Little C. (1992) Periodicity of cambial activity in Abies balsamea. I. Effects of temperature and photoperiod on cambial dormancy and frost hardiness. *Physiologia Plantarum*, **85**, 515-525.

Nardin M., Musch B., Rousselle Y., Guérin V., Sanchez L., Rossi J.-P., Gerber S., Marin S., Pâques L.E. & Rozenberg P. (2015) Genetic differentiation of European larch along an altitudinal gradient in the French Alps. *Annals of Forest Science*, **72**, 517-527.

Park Y.-I. & Spiecker H. (2005) Variations in the tree-ring structure of Norway spruce (*Picea abies*) under contrasting climates. *Dendrochronologia*, **23**, 93-104.

Peters, R.L., Balanzategui, D., Hurley, A.G., Von Arx, G., Prendin, A.L., Cuny, H.E., Björklund, J., Frank, D.C. & Fonti, P. (2018) RAPTOR: row and position tracheid organizer in R. *Dendrochronologia*, **47**, 10-16.

Prendin A.L., Petit G., Carrer M., Fonti P., Björklund J. & von Arx G. (2017). New research perspectives from a novel approach to quantify tracheid wall thickness. *Tree Physiology*, **37**, 976-983.

Proseus T.E., Ortega J.K. & Boyer J.S. (1999) Separating growth from elastic deformation during cell enlargement. *Plant Physiology*, **119**, 775-784.

Proseus T.E., Zhu G.L. & Boyer J.S. (2000) Turgor, temperature and the growth of plant cells: using Chara corallina as a model system. *Journal of Experimental Botany*, **51**, 1481-1494.

R Core Team (2015) R: A language and environment for statistical computing. R Foundation for Statistical Computing, Vienna, Austria. ISBN 3-900051-07-0, URL http://www.R-project.org/.

Rathgeber C.B.K. (2012) Cambial activity and wood formation: data manipulation, visualisation and analysis using R. R package version 1.4-1. http://CRAN.R-project.org/package=CAVIAR.

Rathgeber C.B.K., Cuny H.E. & Fonti P. (2016) Biological basis of tree-ring formation: a crash course. *Frontiers in Plant Science*, **7**, 734.

Rossi S., Anfodillo T., Čufar K., Cuny H.E., Deslauriers A., Fonti P., Frank D., Gričar J., Gruber A., Huang J.-G., Jyske T., Kašpar J., King G., Krause C., Liang E., Mäkinen H., Morin H., Nöjd P., Oberhuber W., Prislan P., Rathgeber C.B.K., Saracino A., Swidrak I. & Treml V. (2016) Pattern of xylem phenology in conifers of cold ecosystems at the Northern Hemisphere. *Global Change Biology*.

Rossi S., Anfodillo T. & Menardi R. (2006a) Trephor: a new tool for sampling microcores from tree stems. *Iawa Journal*, **27**, 89-97.

Rossi S., Deslauriers A. & Anfodillo T. (2006b) Assessment of cambial activity and xylogenesis by microsampling tree species: An example at the alpine timberline. *Iawa Journal*, **27**, 383-394.

Rossi S., Deslauriers A., Anfodillo T. & Carraro V. (2007) Evidence of threshold temperatures for xylogenesis in conifers at high altitudes. *Oecologia*, **152**, 1-12.

Rossi S., Deslauriers A., Gričar J., Seo J.-W., Rathgeber C.B.K., Anfodillo T., Morin H., Levanic T., Oven P. & Jalkanen R. (2008) Critical temperatures for xylogenesis in conifers of cold climates. *Global Ecology and Biogeography*, **17**, 696-707.

Rossi S., Deslauriers A. & Morin H. (2003) Application of the Gompertz equation for the study of xylem cell development. *Dendrochronologia*, **21**, 33-39.

Rossi S., Morin H. & Deslauriers A. (2012) Causes and correlations in cambium phenology: towards an integrated framework of xylogenesis. *Journal of Experimental Botany*, **63**, 2117-2126.

Schoch W., Heller I., Schweingruber F.H. & Kienast F. (2004) Wood anatomy of central European species. Online version: www.woodanatomy.ch.

Schrader J., Baba K., May S., Palme K., Bennett M., Bhalerao R. & Sandberg G. (2003) Polar auxin transport in the wood-forming tissues of hybrid aspen is under simultaneous control of developmental and environmental signals. *Proceedings of the National Academy of Sciences*, **100**, 10096-10101.

Simard S., Giovannelli A., Treydte K., Traversi M.L., King G.M., Frank D. & Fonti P. (2013) Intra-annual dynamics of non-structural carbohydrates in the cambium of mature conifer trees reflects radial growth demands. *Tree Physiology*, **33**, 913-923.

Sutera S.P. & Skalak R. (1993) The history of Poiseuille's law. *Annual Review of Fluid Mechanics*, **25**, 1-20.

Tuominen H., Puech L., Fink S. & Sundberg B. (1997) A radial concentration gradient of indole-3-acetic acid is related to secondary xylem development in hybrid aspen. *Plant Physiology*, **115**, 577-585.

Uggla C., Moritz T., Sandberg G. & Sundberg B. (1996) Auxin as a positional signal in pattern formation in plants. *Proceedings of the National Academy of Sciences of the United States of America*, **93**, 9282-9286.

Vaganov E.A. (1990) The tracheidogram method in tree-ring analysis and its application. In: *Methods of dendrochronology: applications in the environmental sciences* (eds E.R. Cook & L.A. Kairiukstis), pp. 63-76. Kluwer Academic Publishers, Dordrecht, Netherlands.

von Arx G. & Carrer M. (2014) ROXAS - A new tool to build centuries-long tracheid-lumen chronologies in conifers. *Dendrochronologia*, **32**, 290-293.

Wood S.N. (2006) *Generalized additive models: an introduction with R*. Chapman and Hall/CRC, Boca Raton, FL.

Zuur A.F., Ieno E.N., Walker N., Saveliev A.A. & Smith GM. (2009). Mixed effects models and extensions in ecology with R. New York, NY: Springer.

Tables

Table 1. Main characteristics of sites and trees monitored. The table describes the sites (elevation, orientation, mean temperature and number of freezing days over the monitoring period), the trees (age, diameter at breast height [DBH] and height [H]), and the monitoring characteristics (number of years and period of monitoring, species studied, number of sampled trees) for the DNN (Donon, Vosges Mountains, France) and LTAL (Lötschental, Alps, Switzerland) locations. For age, DBH and H, the mean ± the standard deviation are given.

Location	Site	Elevation (m a.s.l.)	Orientation	mean T (°C)	Nb of freezing days	Nb of years	Period of monitoring	Species	Nb of trees per year	Age (year)	DBH (cm)	H (m)
DNN	WAL	370	South-West	10,3	27	3	2007-2009	*Picea abies*	5	89 ± 8	53 ± 4	32 ± 2
	ABR	430	West	9,1	36	3	2007-2009	*Picea abies*	5	85 ± 15	41 ± 5	32 ± 1
	GRA	650	South-East	8,6	39	3	2007-2009	*Picea abies*	5	74 ± 7	55 ± 9	33 ± 3
LTAL	N08	800	North	9,2	64	3	2008-2010	*Larix decidua*	4	167 ± 21	49 ± 5	22 ± 3
								Picea abies	4	154 ± 12	43 ± 9	27 ± 3
	N13	1300	North	5,7	107	7	2007-2013	*Larix decidua*	4	151 ± 18	53 ± 16	31 ± 7
								Picea abies	4	134 ± 40	46 ± 6	27 ± 5
	N13W	1300	North	4,2	123	2	2012-2013	*Larix decidua*	3	153 ± 26	55 ± 14	28 ± 6
								Picea abies	3	111 ± 24	53 ± 16	28 ± 8
	N16	1600	North	4,9	117	4	2007-2010	*Larix decidua*	4	214 ± 33	55 ± 8	33 ± 3
								Picea abies	4	223 ± 64	55 ± 6	34 ± 3
	S16	1600	South	5	113	7	2007-2013	*Larix decidua*	4	152 ± 128	54 ± 12	27 ± 3
								Picea abies	4	221 ± 139	43 ± 9	24 ± 3
	N19	1900	North	3,1	132	4	2007-2010	*Larix decidua*	4	264 ± 20	52 ± 3	32 ± 2
								Picea abies	4	200 ± 25	52 ± 9	30 ± 4
	S19	1900	South	3,9	115	7	2007-2013	*Larix decidua*	4	206 ± 66	43 ± 6	22 ± 2
								Picea abies	4	186 ± 72	50 ± 9	24 ± 3
	N22	2200	North	2,2	152	4	2007-2010	*Larix decidua*	4	251 ± 96	42 ± 9	18 ± 4
	S22	2200	South	3,2	129	7	2007-2013	*Larix decidua*	4	246 ± 39	41 ± 8	18 ± 2

583

584 **Figures**

585

586

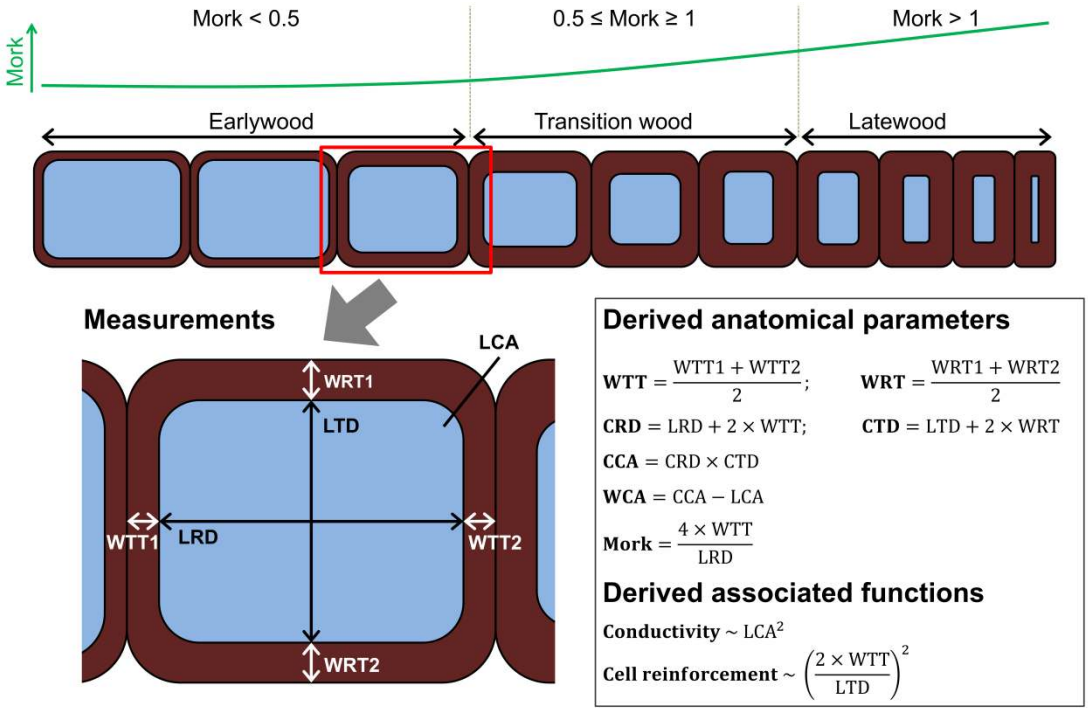

Variable definition
WTT = Tangential wall thickness (µm); **WRT** = Radial wall thickness (µm); **WCA** = Wall cross-sectional area (µm²); **LRD** = Lumen radial diameter (µm); **LTD** = Lumen tangential diameter (µm); **LCA** = Lumen cross-sectional area (µm²); **CRD** = Cell radial diameter (µm); **CTD** = Cell tangential diameter (µm); **CCA** = Cell cross-sectional area (µm²)

587

588

589 **Figure 1. Illustration of the cell anatomical measurements performed.** For every cell
590 along a radial file, we measured the lumen radial and tangential diameter and the cross-
591 sectional area of the lumen, as well as the radial and tangential wall thicknesses. From these
592 measurements, we could then calculate the diameters and area of the cells, and the area of the
593 wall. These dimensions were used to derive some indexes related to cell functional
594 performances, specifically the conductivity and the cell reinforcement (see Methods).

595

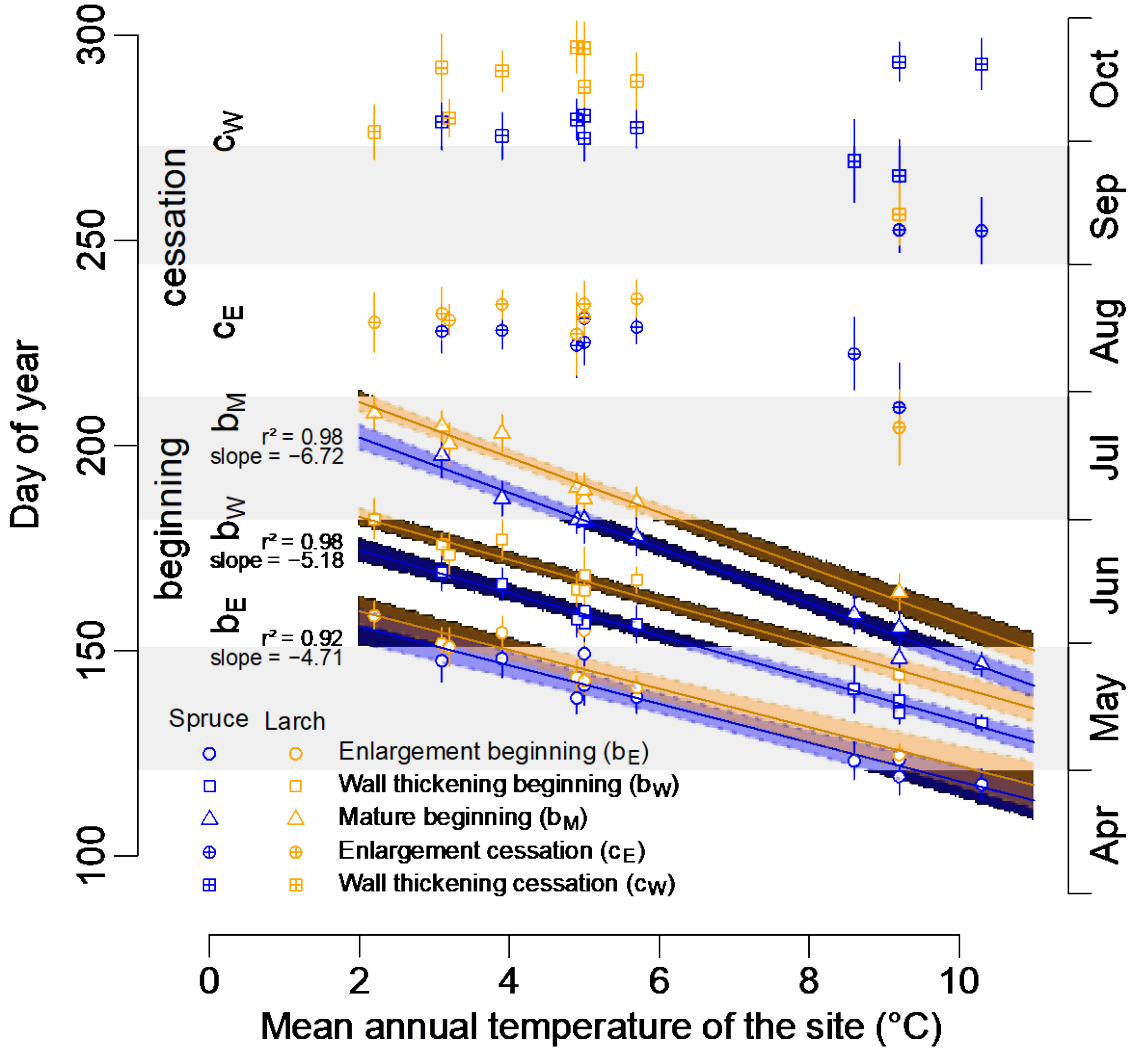

Figure 2. Phenology of wood formation. Timing of xylem tissue formation along the thermal gradient with the beginnings of cell enlargement (b_E), wall thickening (b_W) and mature (b_M) periods and the cessations of cell enlargement (c_E) and wall thickening (c_W) periods. Each point represents a site average for one species, while bar symbolizes the associated standard deviation. Orange and blue lines represent the relationships between air temperature and the different phenological dates for larch and spruce, respectively. Colored areas around lines represent the 95% confidence intervals.

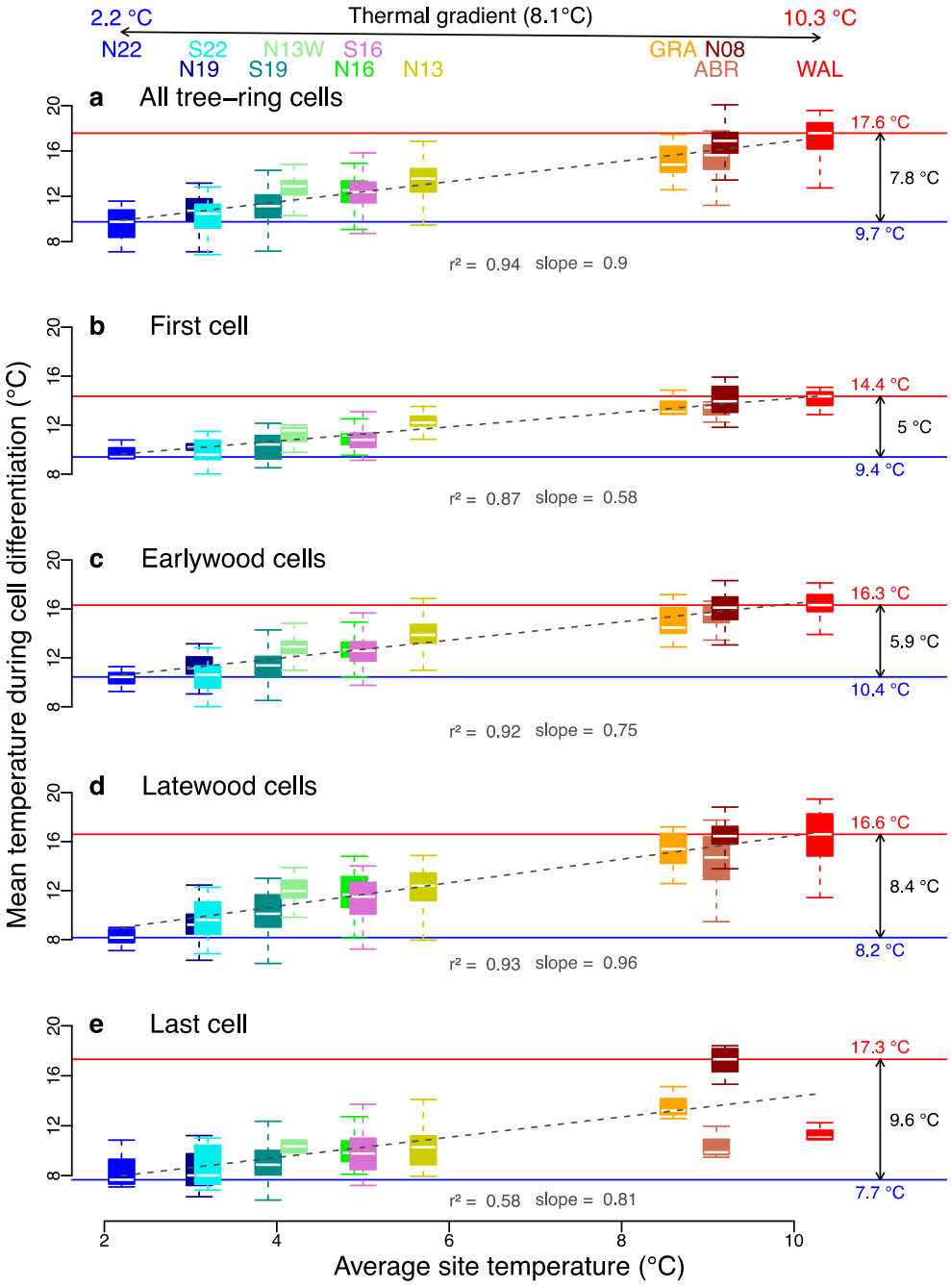

Figure 3. Air temperature experienced during xylem cell differentiation. The figure shows the mean air temperature experienced by xylem cells during their differentiation at the 12 sites along the thermal gradients considering all tree ring cells (**a**), the first cell of the tree-ring (**b**), earlywood cells (**c**), latewood cells (**d**) and the last cell of the tree-ring (**e**). Each boxplot represents the data included in one of the above-mentioned categories for the two species at one site over the monitoring period. The dashed lines represent the relationships between the mean air temperature experienced during xylem cell differentiation and the average site temperature.

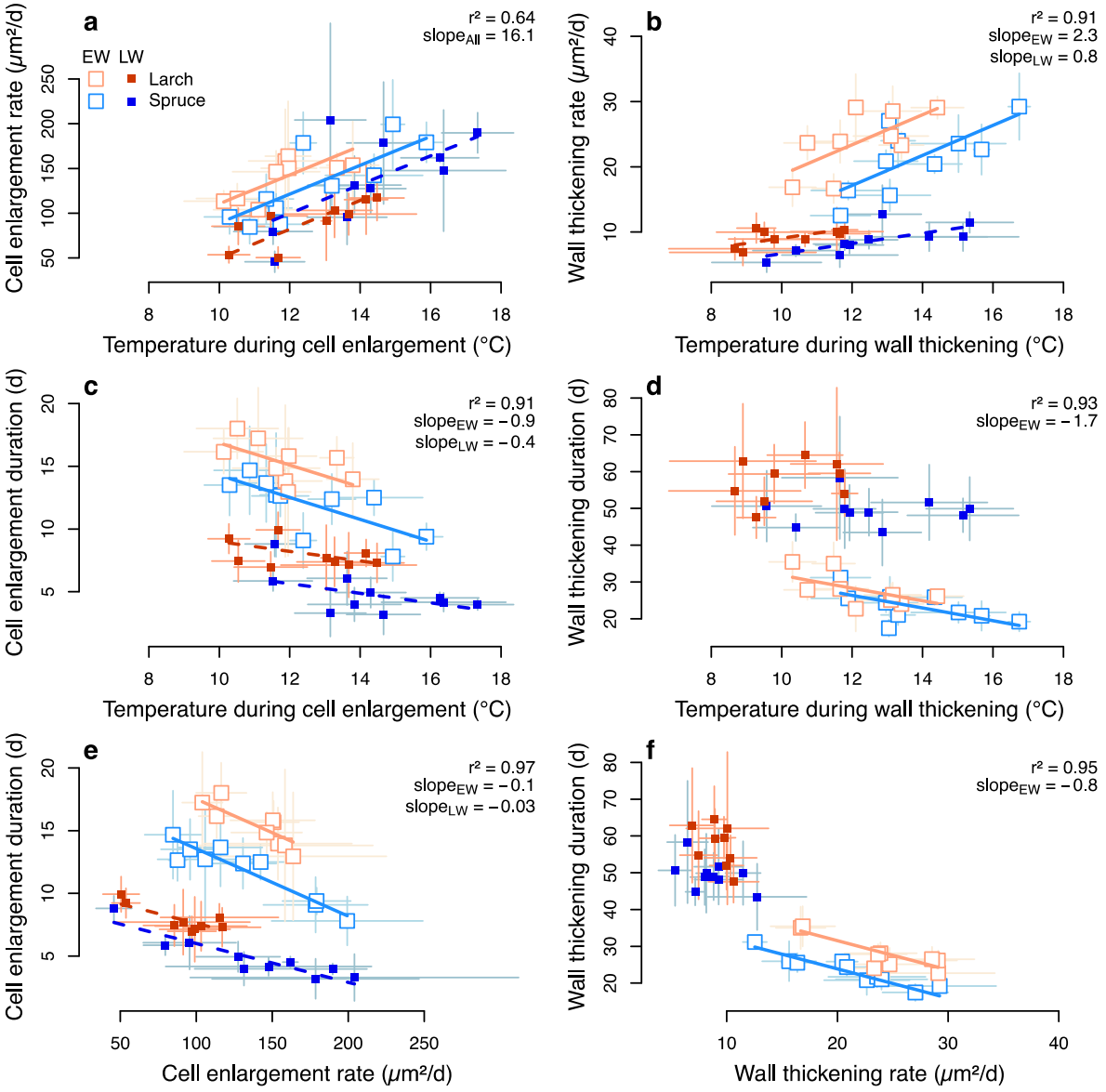

Figure 4. Influence of air temperature on xylem cell kinetics. Relationships between the mean air temperature experienced during process realization and process kinetics, including cell enlargement rate (**a**), wall thickening rate (**b**), cell enlargement duration (**c**) and wall thickening duration (**d**). Relationships between rate and duration of cell enlargement (**e**) and of wall thickening (**f**). Each point represents the site and species average for earlywood (EW) or latewood (LW) cells, with the corresponding 95 % confidence interval. Lines represent the relationships for earlywood (solid light lines) and latewood (dashed dark lines). Slopes of relationships are given separately for earlywood (slope$_{EW}$) and latewood (slope$_{LW}$) when they are different; otherwise a single slope is given (slope$_{All}$). The provided r-squared values are for the whole model.

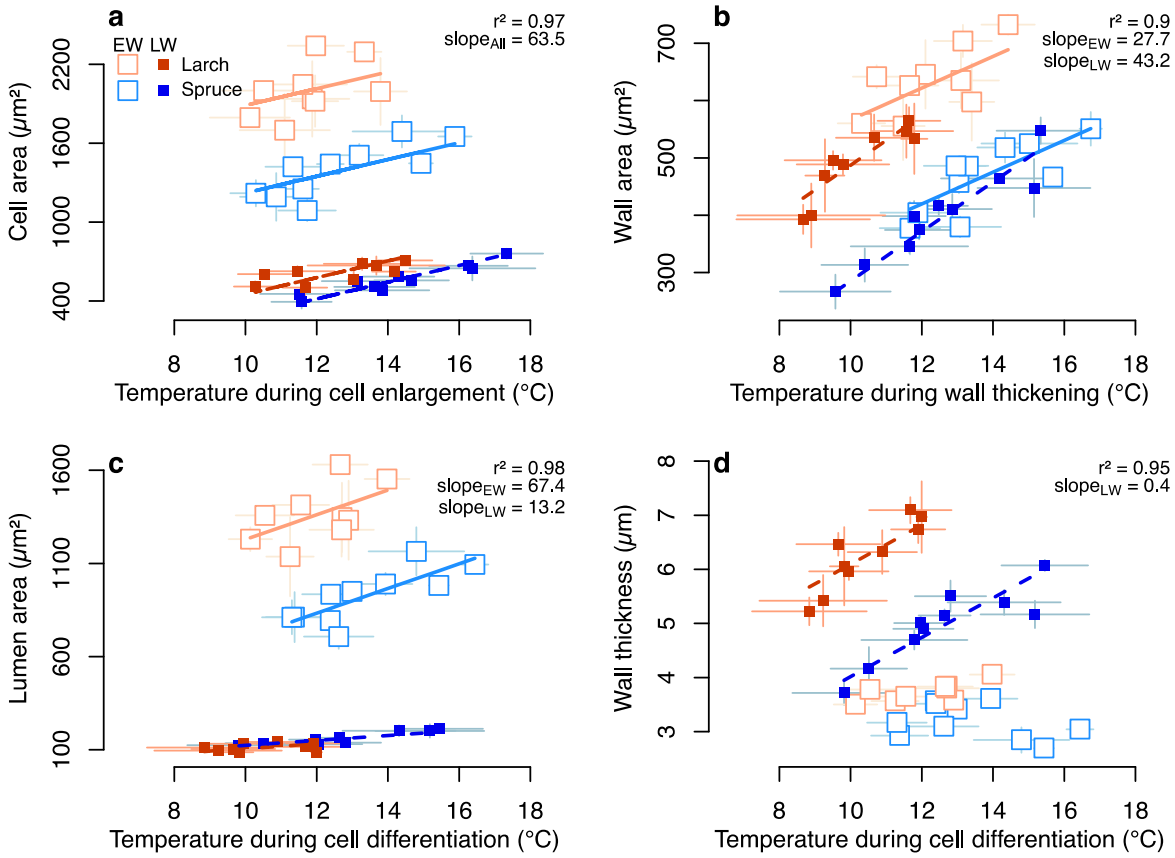

Figure 5. Influence of air temperature on xylem cell dimensions. Relationships between the mean air temperature experienced during process realization and the resulting cell dimension, with the cell cross-sectional area (**a**), the wall cross-sectional area (**b**), the lumen cross-sectional area (**c**) and the wall thickness (**d**). Each point represents the site and species average for earlywood (EW) or latewood (LW) cells, with the corresponding 95 % confidence interval. Lines represent the relationships for earlywood (solid light lines) and latewood (dashed dark lines). Slopes of relationships are given separately for earlywood ($slope_{EW}$) and latewood ($slope_{LW}$) when they are different; otherwise a single slope is given ($slope_{All}$). The provided r-squared values are for the whole model.

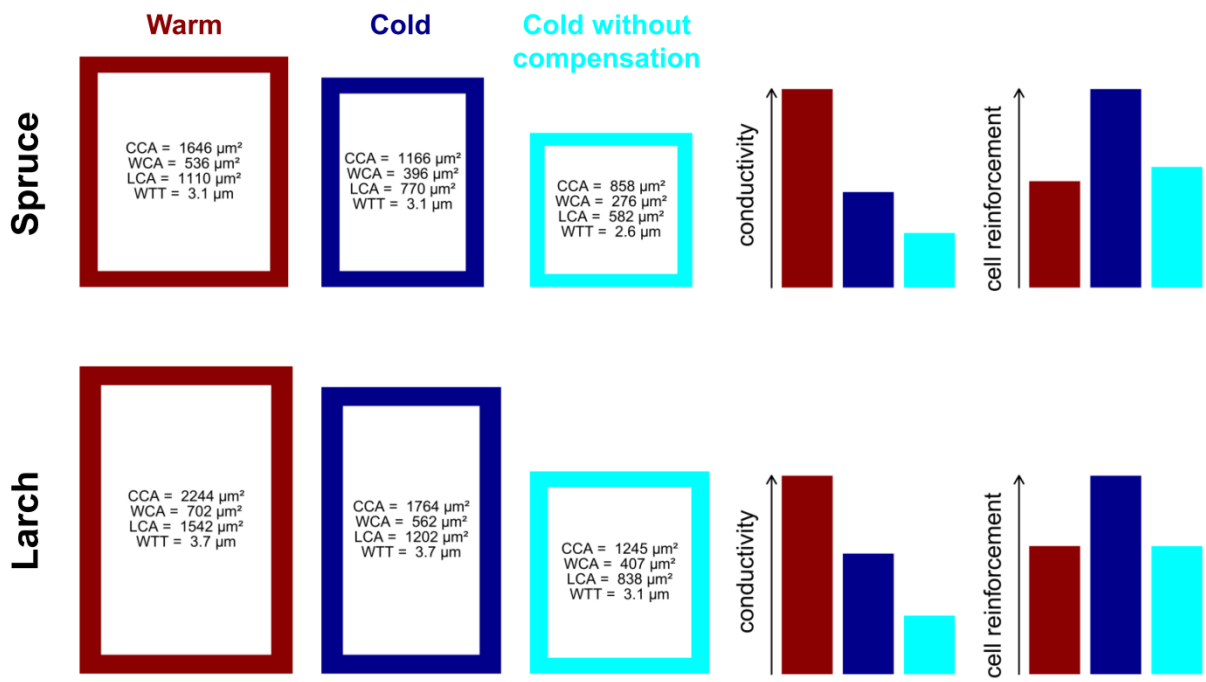

Figure 6. Morphology and associated derived cell functional performance of the earlywood xylem cells produced in European larch and Norway spruce simulated according to three scenarios (warm, cold and cold without compensation). Simulated tracheids were built using the relationships presented in Figure 3 and assuming a 5° C thermal gradient between the "warm" and "cold" scenarios. The "cold without compensation" scenario corresponds to the simulations performed for the theoretical cold site, but using the durations of the theoretical warm site in order to test the effect of the compensation played by the duration on the final cell dimensions and associated functions. The cell, wall and lumen cross-sectional areas (CCA, WCA and LCA), and the tangential wall thickness (WTT) of the simulated tracheids are given.